Aleksa Milovanović<sup>1\*</sup> , Milovan Paunić<sup>2</sup> , Sergiu-Valentin Galaţanu<sup>3</sup> , Ivana Filipović<sup>1</sup> , Miloš Milošević<sup>1</sup> , Liviu Marşavina<sup>3</sup> , Aleksandar Sedmak<sup>2</sup>

# IMPACT PROPERTIES OF FDM-GRADE PLA POLYMER RELATIVE TO INFILL DENSITY UDARNA SVOJSTVA FDM PLA POLIMERA U ODNOSU NA KOLIČINU ISPUNE

Originalni naučni rad / Original scientific paper Rad primljen / Paper received: 1.12.2024 https://doi.org/10.69644/ivk-2025-02-0227

Adresa autora / Author's address:

<sup>1)</sup> University of Belgrade, Innovation Centre of the Faculty of Mechanical Engineering, Belgrade, Serbia

A. Milovanović https://orcid.org/0000-0003-4668-8800, \*email: aleksa753@gmail.com, amilovanovic@mas.bg.ac.rs

I. Filipović <a href="https://orcid.org/0000-0002-7977-2980">https://orcid.org/0000-0002-7977-2980</a>,

M. Milošević https://orcid.org/0000-0002-2418-1032.

<sup>2)</sup> University of Belgrade, Faculty of Mechanical Engineering, Belgrade, Serbia M. Paunić <a href="https://orcid.org/0000-0002-4180-9813">https://orcid.org/0000-0002-4180-9813</a>;

A. Sedmak https://orcid.org/0000-0002-5438-1895

<sup>3)</sup> Department of Mechanics and Strength of Materials, Politehnica University of Timisoara, Timisoara, Romania

S.-V. Galațanu <a href="https://orcid.org/0000-0002-7629-8662">https://orcid.org/0000-0002-7629-8662</a>;

L. Marsavina https://orcid.org/0000-0002-5924-0821

## Keywords

- PLA
- · fused deposition modelling
- · infill density
- · Charpy impact test
- · instrumented pendulum

#### Abstract

This research paper focuses on the influence of infill density on the impact properties of FDM-grade PLA material, i.e., how impact properties degrade with lower infill percentages. Most FDM machines' infill density can vary between 10% and 100%. Here, we include the full infill density spectrum with an increment of 10% (10 specimen groups). The authors' previous research findings show the benefits of smaller layer heights regarding repeatability of results and impact strength values. Thus, the employed layer thickness here is 0.1 mm, the lowest resolution for most FDM machines. Tests were conducted at room temperature and a controlled humidity level of around 50% on the Charpy instrumented pendulum.

#### INTRODUCTION

Additive manufacturing (AM) technologies decrease production time, transforming the prototyping and manufacturing landscape. One of the first introduced AM technologies is fused deposition modelling (FDM), initially intended only for prototyping. However, after some time it also proved useful for manufacturing functional components. Due to such applications, assessing FDM materials' mechanical properties must be of essential importance, /1, 2/. FDM utilises a variety of thermoplastics, with polylactic acid (PLA) being one of the most popular materials globally. PLA is a fully biodegradable material, mainly intended for rapid prototyping. As a thermoplastic, PLA offers sufficient thermal properties necessary for the FDM process, i.e., glass transition and melting temperature of around 60 °C and 200 °C, in respect.

PLA is a recyclable material and cost-effective for most FDM applications which may even include biomedical use due to its scientifically proven biocompatibility, /3/. Nowa-

# Ključne reči

- PLA
- modeliranje deponovanjem topljenog materijala
- količina ispune
- · udarno ispitivanje po Šarpiju
- instrumentalizovano klatno

#### Izvod

Fokus ovog istraživanja je na proceni uticaja količine ispune na udarna svojstva PLA materijala za FDM upotrebu, odnosno, kako udarna svojstva degradiraju sa manjim ispunama. Većina FDM uređaja mogu da naprave delove sa 10 % do 100 % količine ispune. Ovde uzimamo u obzir ceo spektar ispuna sa inkrementom od 10 % (ukupno 10 grupa uzoraka). Prethodna istraživanja autora su pokazala prednosti manjih visina sloja u pogledu ponovljivosti rezultata i vrednosti udarne žilavosti. Stoga, ovde koristimo 0.1 mm za visinu sloja, najmanju za većinu FDM uređaja. Ispitivanja su izvršena na sobnoj temperaturi i pri kontrolisanoj vlažnosti od oko 50 % na Šarpi instrumentiranom klatnu.

days, there is a wide range of engineering applications for PLA materials. Hence, the mechanical behaviour of PLA, especially under dynamic loading conditions, is essential to grasp. In the biomedical field, PLA can be used for the construction of drug delivery systems and bioresorbable implants, /4, 5/.

One of the main features of FDM technology is the potential to manipulate the inside of the component, i.e., the infill structure can have a defined density and pattern. Infill density especially influences FDM part properties, and assessing its influence via experiments is crucial. Low-density infills use less material at the cost of mechanical properties. Still, the optimal infill density that provides enough integrity with less material used depends on the individual application.

The most used mechanical tests include tensile, compressive, and flexural tests, while impact resistance assessment remains relatively underexplored and should be a focus of future research. There are two standardised impact testing procedures: Charpy and IZOD tests. Both methods have

different specimen geometry, but they evaluate the same material property, /6, 7/. Understanding the relationship between different infill densities and material's impact resistance is crucial for the design optimisation of final components. Research on PLA impact properties across a broad range of infill densities remains limited. This research aims to expand this knowledge by testing and analysing the results from a wide range of infill densities, from 10 to 100 %.

Except for experimental impact tests, numerical analysis on PLA components can also be conducted with the help of the ANSYS® finite element software explicit module for impact analysis, named LS-DYNA, /8/. It is important to emphasise that thermoplastic materials exhibit viscoplastic behaviour; hence, the proper constitutive model must be defined in the numerical analysis. For one such case, the 'MCalibration' software is used for material model calibration and tensile test simulation /9/, proving a good correlation between the numerical and experimental results.

The material anisotropy in FDM must not be overlooked because of the layer-by-layer construction of components and non-uniform structure due to nozzle movement during material deposition. Such structures highly depend on angles of material deposition and build orientations, /10/. Hence, the repeatability of results between individual specimens must be considered in the analysis.

Not only infill density but also the infill pattern has a significant effect on mechanical properties of FDM components, /11-14/. The synergy between the infill density and infill patterns is also essential. Material limitations of PLA include brittleness and relatively low impact strength which is challenging for materials' implementation in more advanced applications. Implementation of the PLA material with reinforcements, i.e., carbon fibres /15, 16/, can be a step in the right direction, having the potential to expand PLA's utilisation in new engineering applications.

This research aims to offer a better understanding of how the infill density parameter affects the impact resistance of PLA material while also providing practical recommendations for future research. Hopefully, this study will inspire innovation in AM applications and give readers valuable insights.

## MATERIALS AND METHODS

Charpy specimen geometry follows the recommendations from the ISO 179 standard. Namely, the edgewise single-notched specimens are prepared, having  $80 \times 10 \times 4 \text{ mm}^3$  in bulk and type A notch with a tip radius of 0.25 mm (see Fig. 1). Unlike the conventional method of acquiring the notch (i.e., by machining), here the notch is directly manufactured via the FDM process, as suggested in /17/. The CAD model of the Charpy specimen is created in Solid-Works® (Dassault Systèmes, Vélizy-Villacoublay, France) software and exported in STL format to Simplify3D® (Simplify3D, Cincinnati, OH, USA) slicer software.

The material supplied for this research is pure PLA, socalled 'silk-grey' from the German RepRap company (InnovatiQ GmbH, Kapellenstraße, Feldkirchen, Germany). The main FDM process parameters are given in Table 1. All specimens have a 0.1 mm layer height which has been shown by /18/ to maximise both result repeatability and mechanical performance. Infill density is set from 10 to 100 %, with a 10 % increment, thus including full infill spectra (a total of 10 specimen groups). The considered infill type here is the honeycomb structure which offers overall better mechanical properties than other available patterns in the slicer software used, /19, 20/. Every infill structure is enveloped by two outlines and two top and bottom layers which have a 'rectilinear' raster orientation (see Fig. 2, /21/). All specimen layouts with emphasised infill structures are shown in Fig. 2. The specimens are manufactured with their largest surface facing the build platform, with layers being parallel to the hammer blow direction during the Charpy impact test.

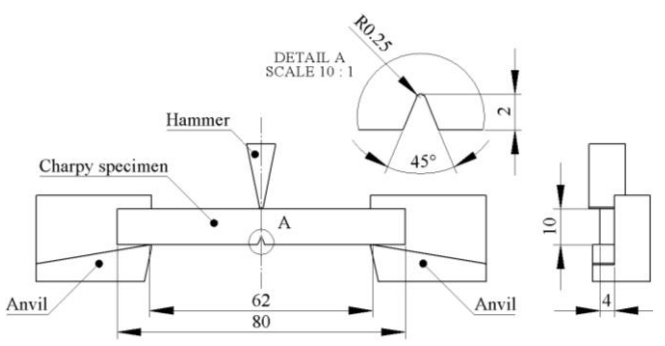
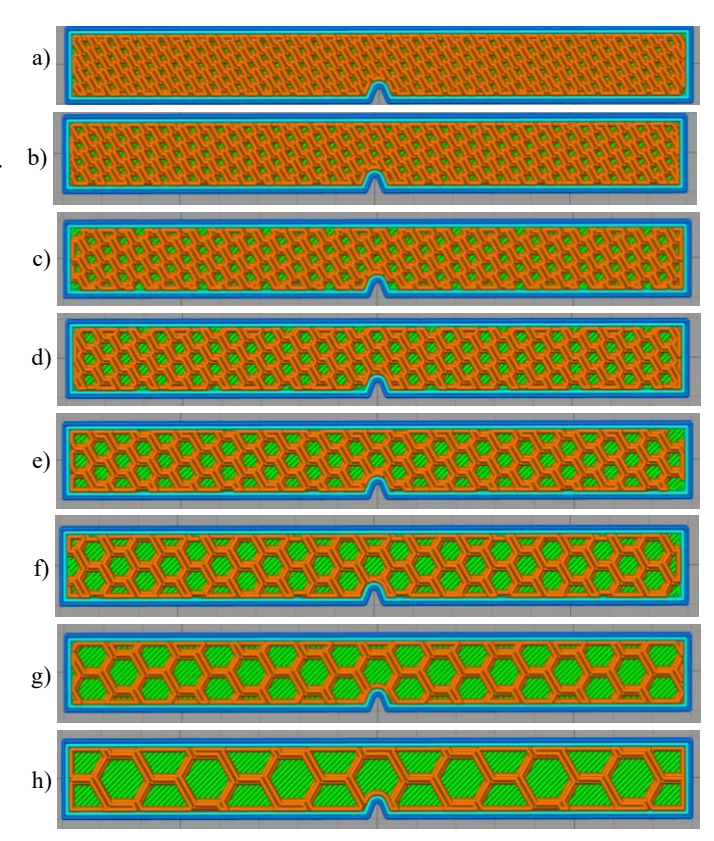


Figure 1. Charpy impact test scheme with loaded specimen.

Table 1. FDM process parameters.

Layer height (mm)	Print speed (mm/s)	Nozzle temp. (°C)	Platform temp. (°C)	Nozzle diameter (mm)
0.1	40	200	60	0.4



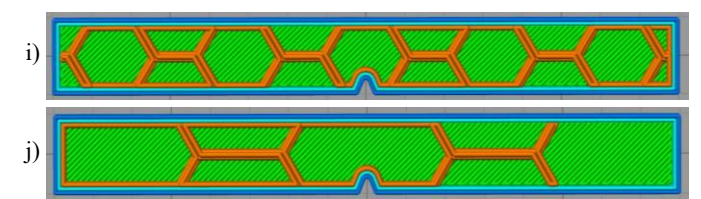


Figure 2. Charpy specimen infill layout: a) 100%; b) 90%; c) 80%; d) 70%; e) 60%; f) 50%; g) 40%; h) 30%; i) 20%; j) 10%.

All Charpy tests were performed on an Instron CEAST 9050 instrumented pendulum, with hammer properties listed in Table 2. The span between the contact points on the anvils is 62 mm (see ISO 179 standard). The machine's sampling rate is set to 1000 Hz, ensuring enough data for analysis. The standard suggests at least five specimens if the repeatability is sufficient. There are seven specimens per test group, with two specimens added for precaution. All specimens are stored and tested at room temperature and a constant humidity level of around 50 %. It is worth noting that all tests were performed on the same day.

Table 2. Instron CEAST 9050 hammer properties.

Potential	Impact	Starting	Weight	Hammer
energy (J)	speed (m/s)	angle (°)	(kg)	length (mm)
5	2.9	150	1.186	229.7

For result visualisation, both MATLAB® and EXCEL® software were used, with MATLAB also being used for the generation of average curves per infill group. Before the result analysis, at least two issues here may come to mind. Firstly, the 100% infill specimens (Fig. 2a) are not fully printed. Namely, there are unfilled spots in the centre of each hexagon, but the highlighted layout is the closest possible to the fully printed part. Secondly, the top and bottom layers with outlines create an envelope around the infill structure, having a discernible share in the 8×4 mm² cross-section at the location of the notch. Therefore, it should come as no surprise if 100% results are of the same order of magnitude with even the lowest infill groups (such as 30% or 20%). The specimen layout for two such cases (i.e., 100% and 20% infill) with an emphasis on cross-section area at the

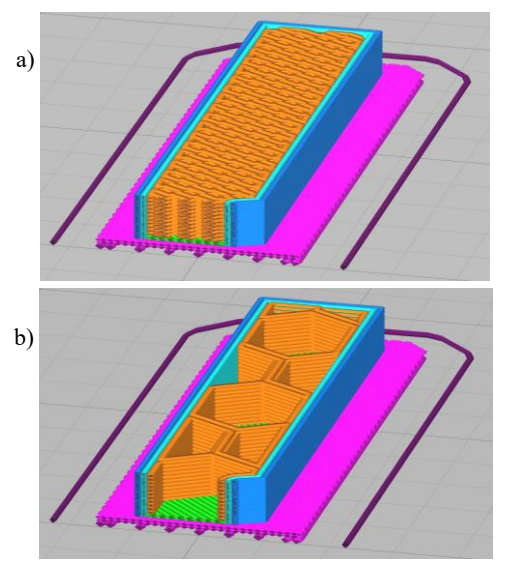


Figure 3. Charpy specimen layout emphasising the cross-section area at the notch: a) for 100 %; b) for 20 % case.

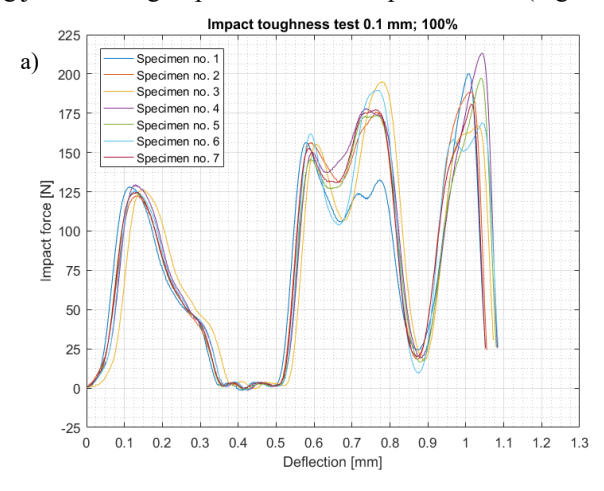
notch (without top layers) is shown in Fig. 3. Specimens' fracture and side surfaces were later observed on a Leica DM6 M optical microscope, providing sharp, high-contrast images with minimal distortion.

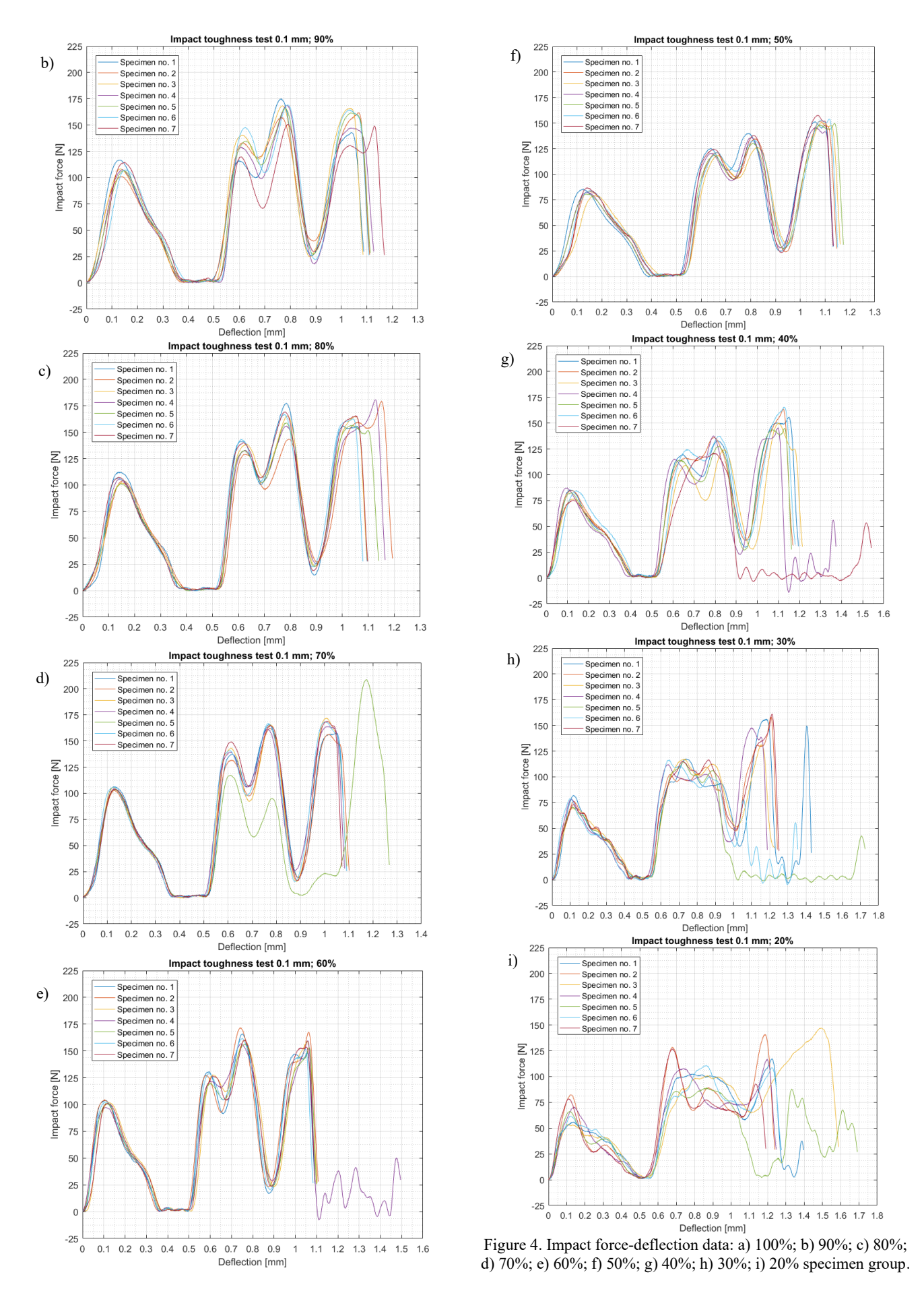
#### RESULTS AND DISCUSSION

All tested specimens had a complete break, i.e., the specimen is separated into two pieces. The impact force-deflection data from all specimen groups are presented in Fig. 4. The mechanical responses from all seven specimens per test group are shown in the images. The 10 % infill group results are excluded from further analysis due to very high data scatter in impact force-deflection response, very high deflection (approx. 5 mm on average), and very low maximal impact force (around 90 N). Due to high deflection values, the impact energy and impact strength are high in the 10 % test group, with values higher than in 100 % infill specimenswhich is undoubtedly an error. Nevertheless, the rest of the data have sufficient repeatability in impact force-deflection response as evident from the nine images below, especially in 100 % to 50 % range. At 40 %, the repeatability is less evident and decreases further in the 30 and 20 % cases. Looking at all tested groups, the repeatability is remarkable in the first conceived peak, with data scatter present only in the last few peaks or at the end of the collected data. One might also observe the low values at the end of the load-deflection response (Figs. 4e, 4g, 4h). This is most likely due to an error in the machine's sensors, i.e., a near-zero response is recorded while the specimen was split in two.

Since all specimens have been broken during the test sequence, the maximal deflection is considered to be the one at the point of specimen break. The maximal deflection value range is between 1 and 1.4 mm, with lower values dedicated to higher infills. Figure 5a shows deflection values per each test group. A shorter chart containing just the test groups with even multiples of ten percent (see Fig. 5b) depicts this trend more clearly.

The inverse trend from deflection data is present in maximal impact force values. Here, higher infills endure higher forces (see Fig. 6a). The highest average value of exactly 195 N is present in the 100 % infill group and descends up to approximately 121 N in the 20 % case, as expected. This decreasing trend from high to low infills is evident when listing just the test groups with even multiples of 10 % (Fig. 6b).





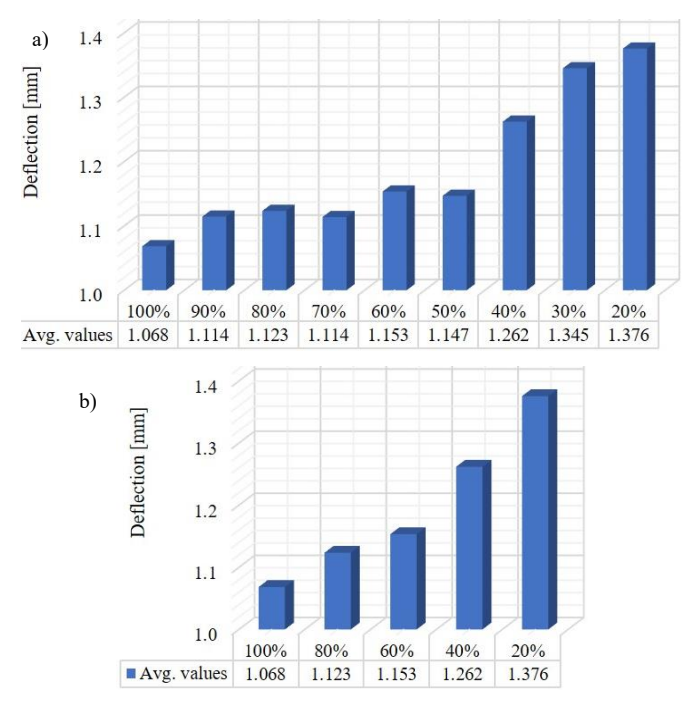


Figure 5. Deflection at break: a) 100 to 20 % values; b) shorter chart with 20 % increment.

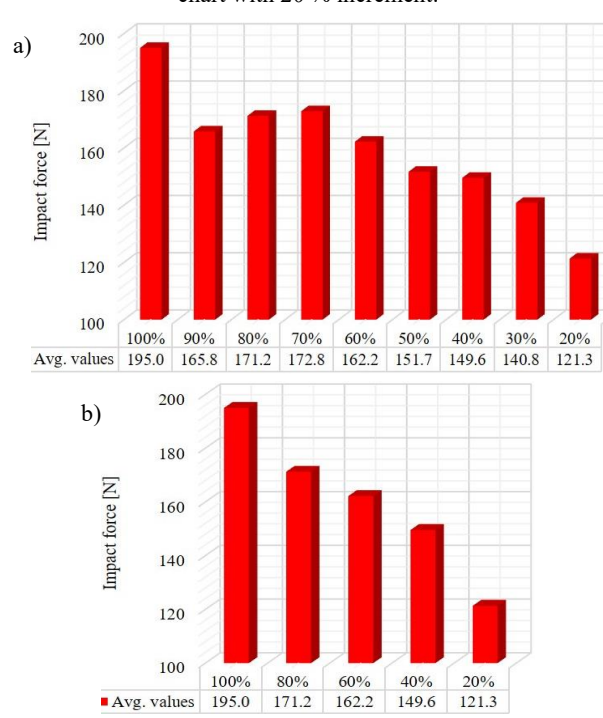
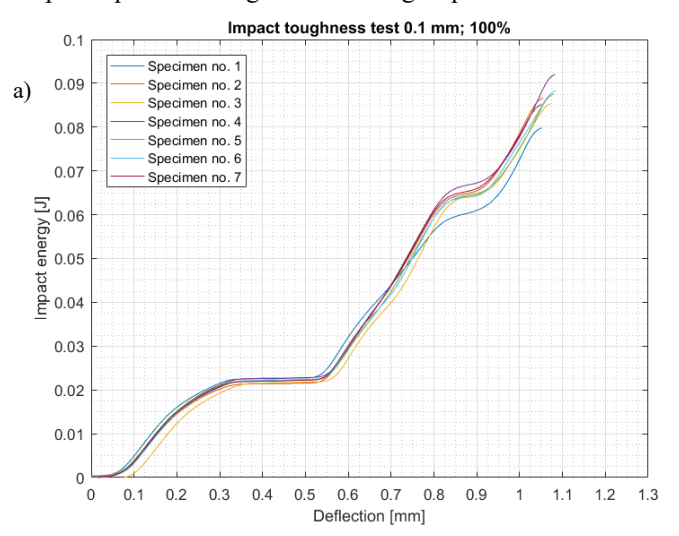
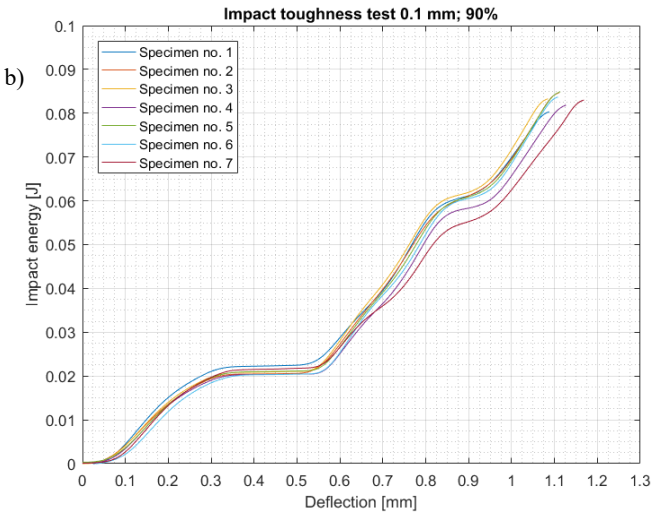


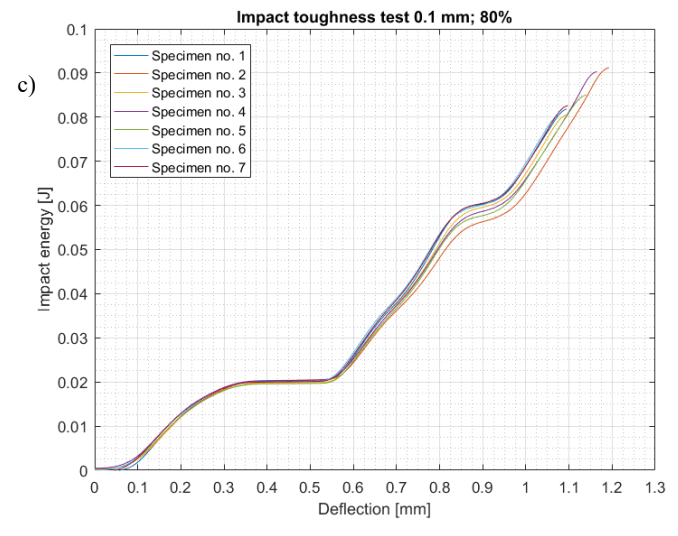
Figure 6. Impact force: a) 100 to 20 % values; b) shorter chart with 20 % increment.

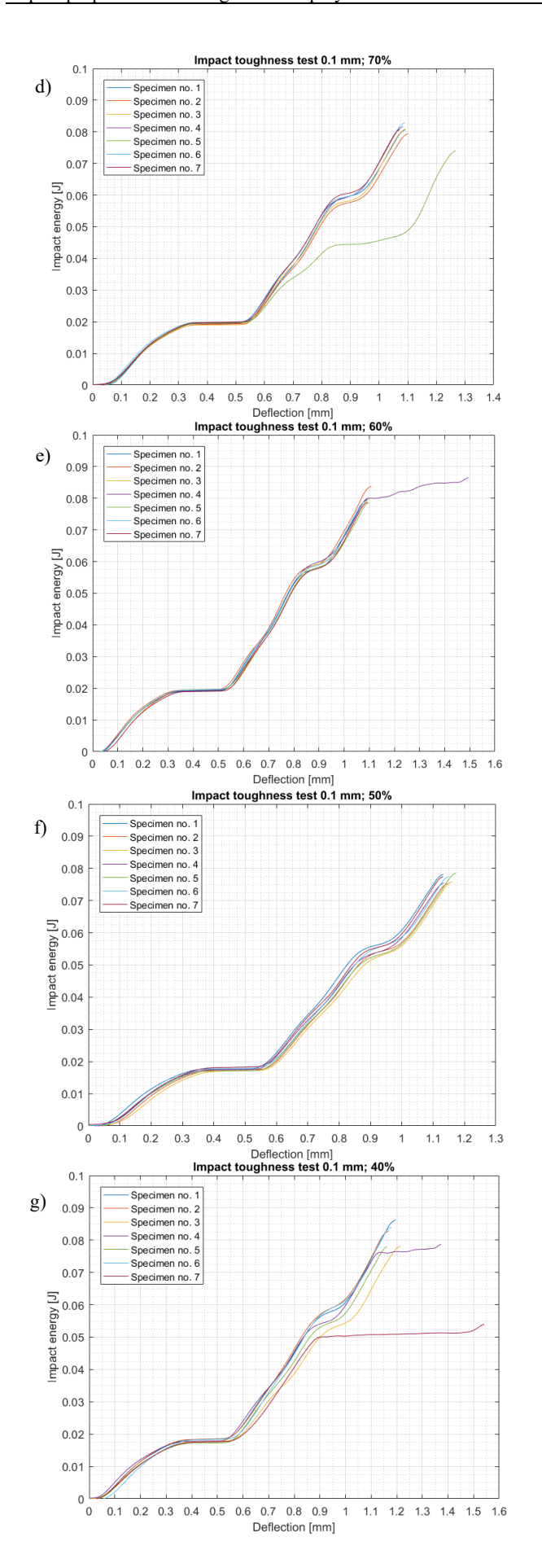
Impact energy-deflection results from all nine considered test groups are shown in Fig. 7. Sufficient repeatability in material response is present from 100 to 50 % specimens, with just one specimen deflecting from the expected response in 70 % case (see Fig. 7d). The plastic deformation (i.e., a location where deflection increases at the constant energy level, /22/) is visible from 0.3 to 0.5 mm, similar to 0.1 and 0.2 mm results with 100 % infill from /18/. The scatter in impact energy-deflection data is visible from 40 % down to 20 %, especially after the performed plastic deformation. The

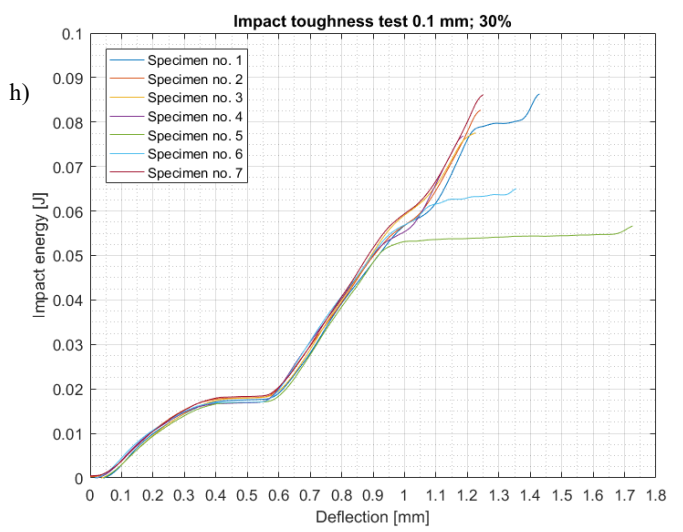
average curves for impact force and impact energy relative to deflection are shown in Fig. 8. In both diagrams, it is visible that the impact force peaks (Fig. 8a) and plastic deformation (Fig. 8b) are similar in shape, with higher material response present in higher infill test groups.











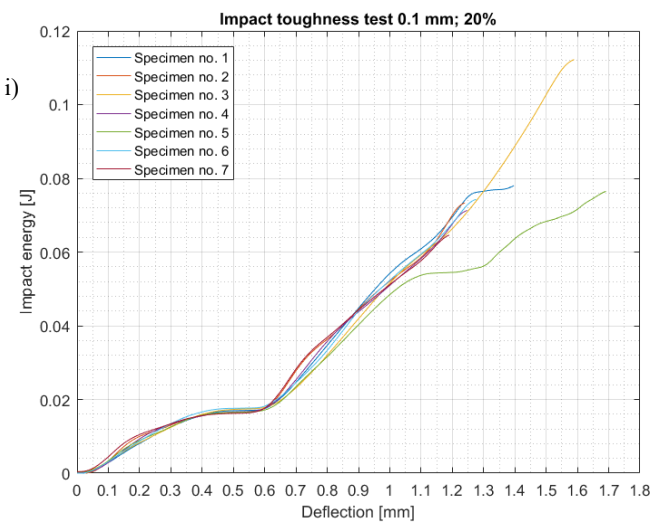
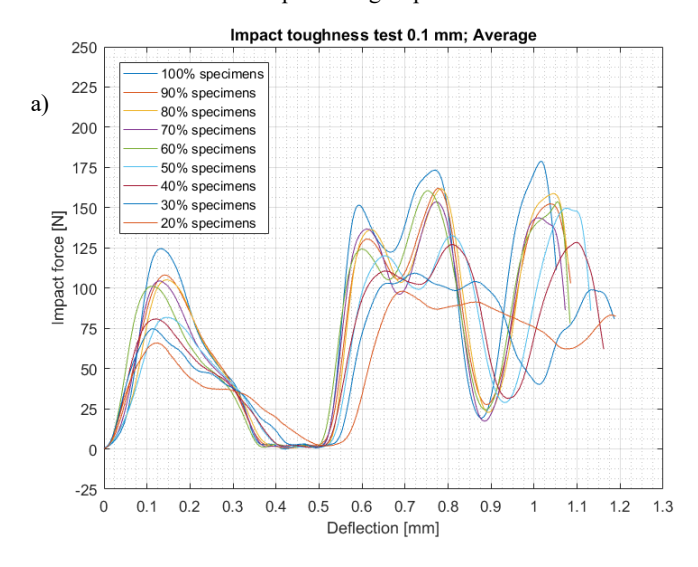


Figure 7. Impact energy-deflection data: a) 100%; b) 90%; c) 80%; d) 70%; e) 60%; f) 50%; g) 40%; h) 30%; i) 20% specimen group.



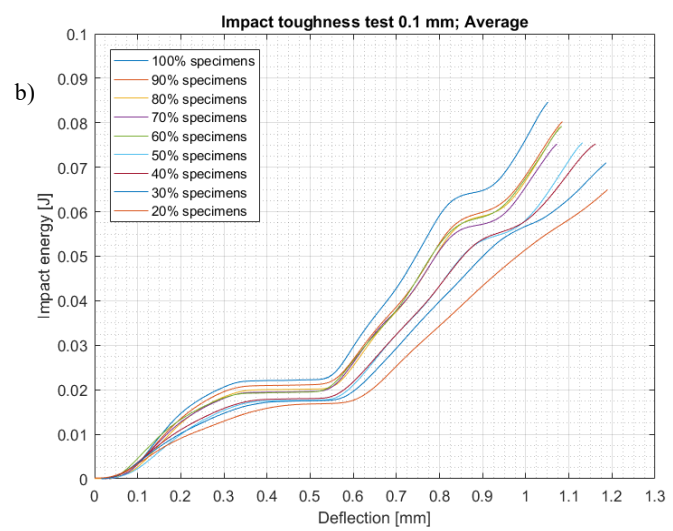


Figure 8. Average curves: a) impact force-deflection; b) impact energy-deflection.

All impact energy results are presented on the chart in Fig. 9a. The maximum impact energy is in the 100 % test

group, with an average value of 86 mJ. The lowest value is in the 30 % group, averaging just below 76 mJ. As can be seen from the shorter chart (Fig. 9b), impact energy values decrease from 100 to 30 %, with some 'recovery' in the 20 % group. This phenomenon is probably due to higher deflection in some specimens from the 20 % batch (Figs. 4i and 7i) since impact energy is calculated from the area underneath the impact force-deflection response. For example, the 10 % results (excluded from further analysis) have a few times greater impact energy values (average is 208.8 mJ) than the rest of the test groups due to considerably higher deflection.

Impact strength values are shown in Fig. 10a. A similar trend as on the impact energy chart is present here due to impact energy values being an integral part of the impact strength equation (see Eq.(2), from section 8.2 in ISO 179-1 standard). Hence, the shorter chart (Fig. 10b) is better for result visualisation. Impact strength values are on the range from 2.2 kJ/m<sup>2</sup> (30 % case) to 2.53 kJ/m<sup>2</sup> (100 % case). Similar recovery as in impact energy results is present in the impact strength results of the 20 % test group, due to the same effect in the 10 % test group (i.e., high deflection).

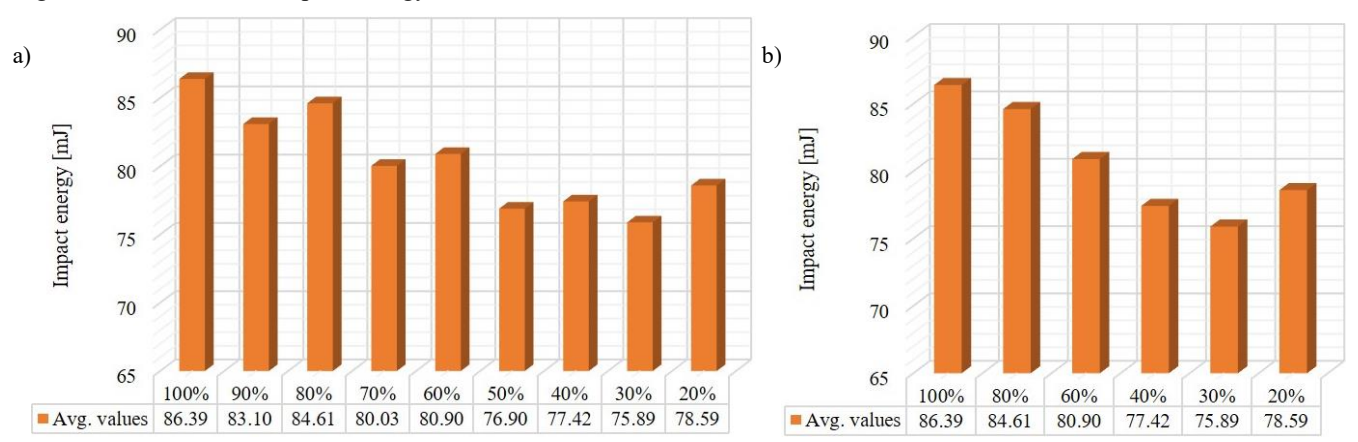


Figure 9. Impact energy: a) 100 to 20 % values; b) shorter chart with 20 % incrementation and 30 % value added.

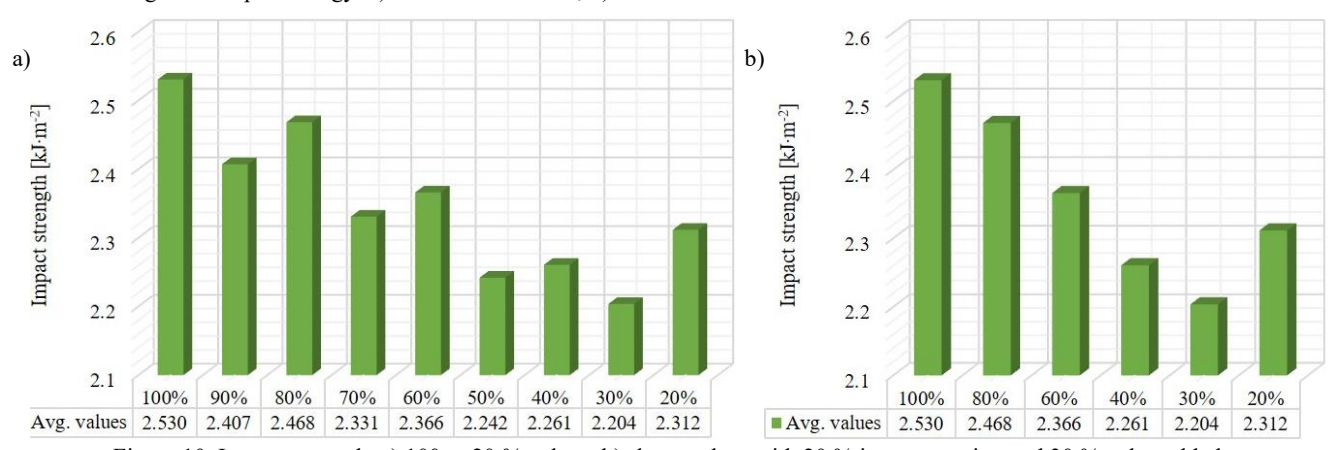


Figure 10. Impact strength: a) 100 to 20 % values; b) shorter chart with 20 % incrementation and 30 % value added.

Fracture surfaces for four different infill density cases (100 %, 70 %, 40 %, and 10 %) are shown in Fig. 11. Each specimen is split in two during the Charpy test, and the images depict only one half of each specimen. The notch is positioned at the bottom of each image, as indicated in Fig. 11a. Bright white regions are visible across all specimens in Fig. 11, indicating areas where the material has undergone

significant deformation before fracture, /23, 24/. Unfilled areas of the honeycomb structure are also visible, appearing as hollow stripes, highlighted by the red lines that encompass these features in Fig. 11a. The 10 % infill density specimen (Fig. 11d) shows almost no internal structure, making it easier to observe the size and portion of the outer layers in the full volume.

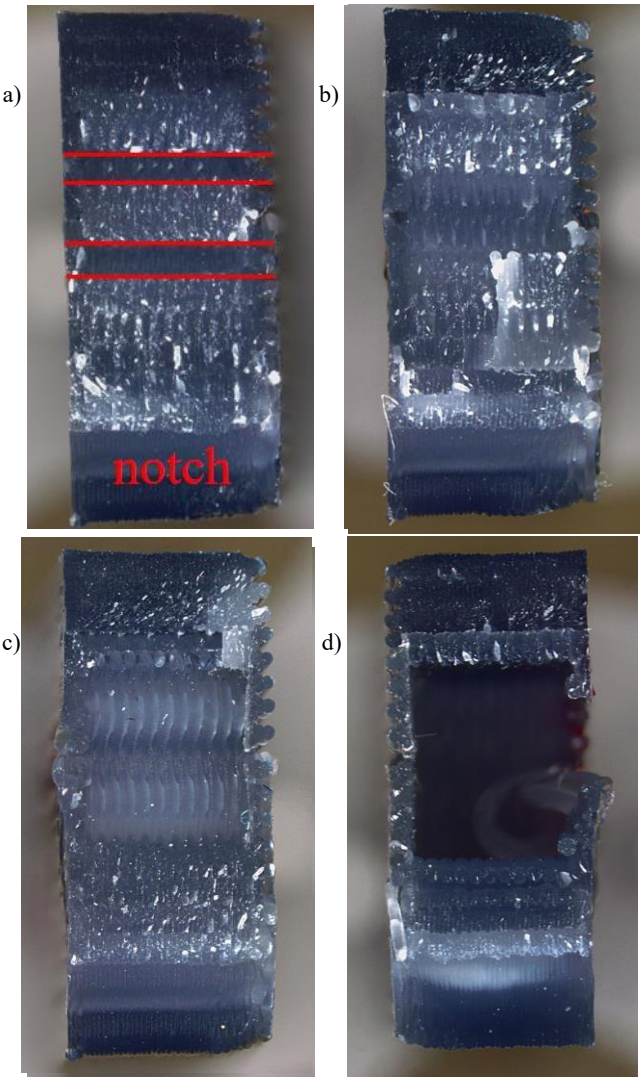


Figure 11. Fracture surfaces: a) 100 %; b) 70 %; c) 40 %; d) 10 %.

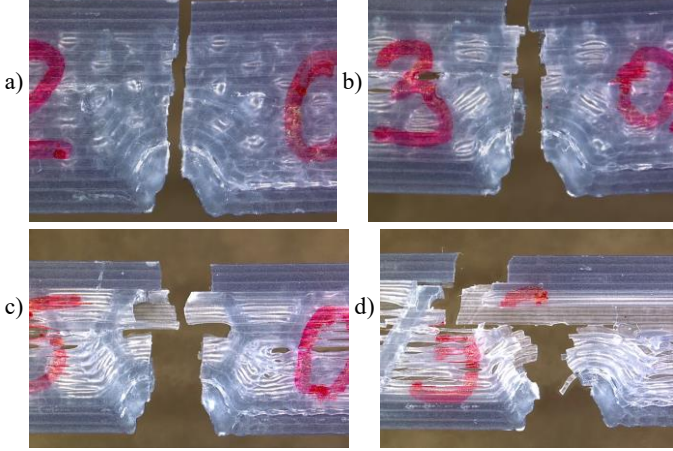


Figure 12. Side surfaces: a) 100%; b) 70%; c) 40%; d) 10%.

Side surfaces are also examined under the same setting as in the previous figure (Fig. 12). In these images, it is clear that specimens with higher infill densities exhibit a clean, straight cut through the ligament (Figs. 12a-b). In contrast, specimens with lower infill densities have raster lines that protrude in both halves of the specimen (Figs. 12c-12d). The

straightest cut is observed in the 100 % infill specimen (Fig. 12a), while the most noticeable protrusions are seen in 10 % infill density specimens (Fig. 12d).

### **CONCLUSIONS**

The main objective of this research is to evaluate the influence of infill density on the impact properties of FDM-grade pure PLA material. The full infill spectrum is considered, i.e., from 100 % down to 10 %, with a 10 % increment. All specimens have a 0.1 mm layer height since it proved to be the best considering result repeatability and mechanical response, as proven in previous research /18/ which considers different layer heights. Unfortunately, the 10 % results are excluded from further analysis due to very high deflection values which influence the creation of erroneous impact energy and impact strength values.

The impact force and impact energy results relative to deflection show significant repeatability in higher infill groups (i.e., from 100 % to 50 %), and there is some distortion in the lower infill groups (i.e., 40 %, 30 %, and 20 %). From average curves, it is clear that higher infill groups have a higher mechanical response, with all test groups having similar shapes in impact force peaks and plastic deformation (visible on impact energy-deflection diagrams). All Charpy specimens experienced a complete break, with specimen separating in two pieces at the notch. The deflection at break, maximal impact force, impact energy, and impact strength are also considered in the analysis, proving benefits in the overall results of higher infills. An intriguing observation is that some test groups with even multiples of 10 % (such as 60 %) exhibit higher impact energy and, consequently, higher impact strength than the subsequent test group (in this case, 70 %). This phenomenon can be explained by the deflection (Fig. 5) and impact force (Fig. 6) charts. Specifically, the lower infill density groups, such as the 60 % group, exhibit higher deflection compared to the 70 % group, despite impact forces being more similar in value. Consequently, the 60 % group demonstrates higher impact energy and impact strength than the 70 % group.

All impact strength values are of the same order of magnitude which is unexpected since the lower infill density specimens have considerably less material. This can be attributed to the influence of the top and bottom layers surrounding the infill, along with the outlines which are at least 1 mm thick. The envelope impacts the results similar to that in /25/, particularly since the cross-section at the notch here is only 8×4 mm². The suggestion is to consider non-standard Charpy specimens, much larger in volume, to shrink the effect of this encirclement on impact results. Given the high sensitivity and precision of the Charpy instrumented pendulum, excluding the envelope could negatively impact the repeatability of the results due to variations in the infill geometry.

### **ACKNOWLEDGEMENTS**

The authors would like to thank the support from the Ministry of Science, Technological Development and Innovation of the Republic of Serbia, under contract No.451-03-136/2025-03/200213 (from February 4, 2025).

## REFERENCES

- Khosravani, M.R., Berto, F., Ayatollahi, M.R., Reinicke, T. (2020), Fracture behavior of additively manufactured components: A review, Theor. Appl. Fract. Mech. 109: 102763. doi: 10.1016/j.tafmec.2020.102763
- Ngo, T.D., Kashani, A., Imbalzano, G., et al. (2018), Additive manufacturing (3D printing): A review of materials, methods, applications and challenges, Comp. Part B: Eng. 143: 172-196. doi: 10.1016/j.compositesb.2018.02.012
- Silva, D., Kaduri, M., Poley, et al. (2018), Biocompatibility, biodegradation and excretion of polylactic acid (PLA) in medical implants and theranostic systems, Chem. Eng. J, 340: 9-14. doi: 10.1016/j.cej.2018.01.010
- Singhvi, M.S., Zinjarde, S.S., Gokhale, D.V. (2019), Polylactic acid: synthesis and biomedical applications, J Appl. Microbiol. 127(6): 1612-1626. doi: 10.1111/jam.14290
- Tyler, B., Gullotti, D., Mangraviti, A., et al. (2016), Polylactic acid (PLA) controlled delivery carriers for biomedical applications, Adv. Drug Deliv. Rev. 107: 163-175. doi: 10.1016/j.addr .2016.06.018
- Popa, C.F., Mărghitaş, M.P., Galațanu, S.V., Marşavina, L. (2022), Influence of thickness on the IZOD impact strength of FDM printed specimens from PLA and PETG, Procedia Struct. Integr. 41: 557-563. doi: 10.1016/j.prostr.2022.05.064
- Ailinei, I.-I., Galaţanu, S.V., Marşavina, L. (2021), The effects of layers orientation on impact energy evaluation of FDM printed specimens, Mater. Des. Process. Comm. 3(6): e267. doi: 10.10 02/mdp2.267
- 8. Popa, C.F., Krausz, T., Galatanu, S.V., et al. (2023), Numerical and experimental study for FDM printed specimens from PLA under IZOD impact tests, Mater. Today: Proc. 78(Part 2): 326-330. doi: 10.1016/j.matpr.2022.11.501
- Milovanović, A., Sedmak, A., Paunić, M., et al. (2024), Tensile properties of pure PLA polymer dedicated for additive manufacturing, Struct. Integr. Life, 24(3): 263-268. doi: 10.69644/ivk-2024-03-0263
- Stoia, D.I., Galațanu, S.V., Marşavina, L. (2022), Impact properties of laser sintered polyamide, according to building orientation, J Mech. Sci. Technol. 37(6): 1119-1123. doi: 10.1007/s 12206-022-2108-0
- Birosz, M.T., Ledenyák, D., Andó, M. (2022), Effect of FDM infill patterns on mechanical properties, Polym. Test. 113: 107654. doi: 10.1016/j.polymertesting. 2022.107654
- Eryildiz, M. (2021), The effects of infill patterns on the mechanical properties of 3D printed PLA parts fabricated by FDM, Ukrain. J Mech. Eng. Mater. Sci. 7(1-2): 1-8. doi: 10.23939/uj mems2021.01-02.001
- 13. Tanveer, M.Q., Mishra, G., Mishra, S., Sharma, R. (2022), Effect of infill pattern and infill density on mechanical behaviour of FDM 3D printed Parts- a current review, Mater. Today: Proc. 62(Part 1): 100-108. doi: 10.1016/j.matpr.2022.02.310
- 14. Pandžić, A., Hodžić, D., Milovanović, A. (2019), Effect of infill type and density on tensile properties of PLA material for FDM process, In: B. Katalinić (Ed.), Proc. 30th DAAAM Int. Symp. on Intelligent Manuf. and Automation, pp.0545-0554. Publ. by DAAAM Int., Vienna, Austria. doi: 10.2507/30th.daaam.proce edings.074
- Valvez, S., Santos, P., Parente, J.M., et al. (2020), 3D printed continuous carbon fiber reinforced PLA composites: A short review, Procedia Struct. Integr. 25: 394-399. doi: 10.1016/j.pro str. 2020.04.056
- Wang, A., Tang, X., Zeng, Y., et al. (2024), Carbon fiber-reinforced PLA composite for fused deposition modeling 3D printing, Polymers, 16(15): 2135. doi: 10.3390/polym16152135

- 17. Vălean, C., Marşavina, L., Mărghitaş, M., et al. (2020), The effect of crack insertion for FDM printed PLA materials on Mode I and Mode II fracture toughness, Procedia Struct. Integr. 28(10): 1134-1139. doi: 10.1016/j.prostr.2020.11.128
- Milovanović, A., Galaţanu, S.V., Sedmak, A., et al. (2024), Layer thickness influence on impact properties of FDM printed PLA material, Procedia Struct. Integr. 56(1): 190-197. doi: 10. 1016/j.prostr.2024.02.055
- 19. Jerez-Mesa, R., Travieso-Rodriguez, J.A., Llumà-Fuentes, J., et al. (2017), *Fatigue lifespan study of PLA parts obtained by additive manufacturing*, Procedia Manuf. 13: 872-879. doi: 10.1016/j.promfg.2017.09.146
- Travieso-Rodriguez, J.A., Zandi, M.D., Jerez-Mesa, R., Llumà-Fuentes, J. (2020), Fatigue behavior of PLA-wood composite manufactured by fused filament fabrication, J Mater. Res. Technol. 9(4): 8507-8516. doi: 10.1016/j.jmrt.2020.06.003
- Milovanović, A., Golubović, Z., Kirin, S., et al. (2023), Manufacturing parameter influence on FDM polypropylene tensile properties, J Mech. Sci. Technol. 37(11): 5541-5547. doi: 10.1 007/s12206-023-2305-5
- Krausz, T., Ailinei, I.-I., Galaţanu, S.V., Marşavina, L. (2021), Charpy impact properties and numerical modeling of polycarbonate composites, Mater. Des. Process. Comm. 3(4): e260. doi: 10.1002/mdp2.260
- Spoerk, M., Arbeiter, F., Cajner, H., et al. (2017), Parametric optimization of intra- and inter-layer strengths in parts produced by extrusion-based additive manufacturing of poly(lactic acid), J Appl. Polym. Sci. 134(41): 45401. doi: 10.1002/app.45401
- Arbeiter, F., Spoerk, M., Wiener, J., et al. (2018), Fracture mechanical characterization and lifetime estimation of nearhomogeneous components produced by fused filament fabrication, Polym. Test. 66: 105-113. doi: 10.1016/j.polymertesting.2 018 01 002
- Popa, C.F., Krausz, T., Galatanu, S.V., Marsavina, L. (2024), *The influence of contour on FDM parts for the Shear Test*, Procedia Struct. Integr. 56: 176-183. doi: 10.1016/j.prostr.2024.02. 053
- © 2025 The Author. Structural Integrity and Life, Published by DIVK (The Society for Structural Integrity and Life 'Prof. Dr Stojan Sedmak') (<a href="http://divk.inovacionicentar.rs/ivk/home.html">http://divk.inovacionicentar.rs/ivk/home.html</a>). This is an open access article distributed under the terms and conditions of the <a href="https://creative.commons.org/">Creative.commons</a> <a href="https://creative.commons.org/">Attribution-NonCommercial-NoDerivatives 4.0 International License</a>